Journal of Solid State Chemistry **156,** 213–219 (2001)
doi:10.1006/jssc.2000.8984, available online at http://www.idealibrary.com on IDEAL®

Syntheses, Structures, and Thermal Expansion of Germanium Pyrophosphates

Enrique R. Losilla, Aurelio Cabeza, Sebastián Bruque, Miguel A. G. Aranda,[1] Jesús Sanz,* Juan E. Iglesias,* and José A. Alonso*

*Departamento de Química Inorgánica, Cristalografía y Mineralogía, Universidad de Málaga, 29071 Málaga, Spain; and *Instituto de Ciencia de Materiales, CSIC, Cantoblanco, 28049 Madrid, Spain*

Received June 29, 2000; in revised form September 1, 2000; accepted October 3, 2000; published online January 3, 2001

α-$Ge(HPO_4)_2 \cdot H_2O$ has been hydrothermally prepared and its thermal behavior has been studied by DTA and thermodiffractometry. Three pyrophosphates can be obtained on heating at high temperature. α-GeP_2O_7 is protocrystalline with a layered structure related to that of the pristine material. α-GeP_2O_7 transforms to β-GeP_2O_7 above 950°C and this yields γ-GeP_2O_7 above 1000°C. However, γ-GeP_2O_7 could not be prepared as single phase at high temperature and ambient pressure because P_2O_5 is partly released leading to a contamination with $Ge_5O(PO_4)_6$ which is the final thermal decomposition product. γ-GeP_2O_7 has been synthesized as a single phase by heating α-GeP_2O_7 at 20 kbar and 1000°C. γ-GeP_2O_7, previously reported as cubic, is monoclinic with $a = 22.8647(4)$ Å, $b = 22.8783(4)$ Å, $c = 22.9429(4)$ Å, $\beta = 90.328(1)°$, $V = 12001.3(4)$ Å^3 and symmetry $P2_1/c$ or lower. γ-GeP_2O_7, with a simple stoichiometry, crystallizes in a very large unit cell with at least 26 Ge, 54 P, and 190 O crystallographically independent atoms. This complex superstructure is caused by the ordered pattern of the P–O–P bent groups. The ^{31}P MAS-NMR profiles of γ-GeP_2O_7, β-GeP_2O_7, and $Ge_5O(PO_4)_6$ are reported and discussed. The thermal expansion of γ-GeP_2O_7 is also described.

Key Words: **low thermal expansion materials; superstructure; powder diffraction.**

INTRODUCTION

There is a recent interest in $M^{IV}X^{V}_2O_7$ (M = Si, Ge, Sn, Pb, Ti, Zr, Hf, Mo, W, Re, Ce, Th, U; X = P, V, As) compounds and their solid solutions because they may present isotropic negative thermal expansion for some compositions in the appropriate temperature intervals (1). There is also general agreement in that $M^{IV}P_2O_7$ crystallizes in a cubic structure with $Z = 4$, $a \sim 8$ Å, that was solved (2) for M = Zr from powder X-ray diffraction data in space group $Pa\bar{3}$. Studying Weissenberg pictures of a GeP_2O_7 single crystal (3), a $3 \times 3 \times 3$, $Z = 108$, supercell was found that was also cubic within experimental error of that time. A careful study of the powder patterns for M = Si, Sn, Pb, Ti, Zr, Hf, and U compounds also showed similar supercells (3, 4); these supercells were confirmed for M = Ge, Zr, and U by indexing of Guinier-Hägg photographs taken with strictly monochromatic Cu$K\alpha_1$ radiation (4).

A landmark in the study of these compounds was the $3 \times 3 \times 3$ superstructure determination of SiP_2O_7 from single crystal data [$a = 22.418$ Å, $Pa\bar{3}$] (5). Similar cubic superstructures have recently been described from Rietveld refinements for MP_2O_7 (M = Zr, (6) Ti (7)) and from single crystal data for ZrV_2O_7 (8). However, we are aware that the situation may be more complex as synchrotron X-ray single crystal data for MoP_2O_7 showed $3 \times 3 \times 3$ superstructure peaks that were indexed in a metrically cubic lattice but with lower symmetry, probably orthorhombic (9). Unfortunately, this huge complex structure could not be solved. The description of the MP_2O_7 structure in the cubic subcell, $a \sim 8$ Å, requires all the pyrophosphate, P–O–P, groups to be linear which it is energetically very unfavorable. In the cubic superstructure description, most (89%) P–O–P bonds are bent to angles ranging between 140° and 150°, while the remaining 11% P–O–P are described as linear, due to both P and the bridging oxygen atoms are lying on a threefold axis of rotation. The thermal vibration parameters of the bridging oxygens of linear P–O–P groups have much higher values than those of the remaining bent bridging oxygens. These high B-values indicate either high thermal anisotropic vibration or positional disorder or even a wrong description of the symmetry of the structure. The developing of a cubic $3 \times 3 \times 3$ superstructure partially relaxes the structure but there remains an internal stress as the linear P–O–P groups are not stable. It is interesting to remark that the metrically cubic orthorhombic diffraction pattern observed (9) for MoP_2O_7 would be compatible with a

[1] To whom correspondence should be addressed. E-mail: g_aranda@uma.es.

0022-4596/01 $35.00

structure having all P–O–P groups bent, provided that it is acentric (1).

A very stable compound in the GeO_2–P_2O_5 system (10) at high temperature is $Ge_5O(PO_4)_6$. Its crystal structure was determined from single-crystal data (11). The thermal decomposition pathway for α-$Ge(HPO_4)_2 \cdot H_2O$ has been reported (12). α-$Ge(HPO_4)_2 \cdot H_2O$ changes to $Ge(HPO_4)_2$ above 230°C and subsequently to α-GeP_2O_7 at 480°C. α-GeP_2O_7 transforms to the β polymorph on heating above 930°C and β-GeP_2O_7 changes to γ-GeP_2O_7 above 1020°C. Finally, γ-GeP_2O_7 decomposes near to 1160°C, releasing P_2O_5. α-GeP_2O_7 has very low crystallinity and even its unit cell is not known. β-GeP_2O_7 is triclinic ($V = 232.8$ Å^3, $\rho_{cryst} = 3.52$ g/cc) and the structure was solved from single-crystal data (13). γ-GeP_2O_7 was reported to be cubic with the early mentioned $3 \times 3 \times 3$ superstructure (3, 4, 10). γ-GeP_2O_7 has slightly higher density, ($V = 11946$ Å^3, $\rho_{cryst} = 3.70$ g/cc) and the atomic positional parameters have not been reported.

Our main interest in studying γ-GeP_2O_7 is to characterize its thermal behavior and to compare it with those shown by cubic MP_2O_7. Hence, X-ray powder diffraction and ^{31}P MAS-NMR spectroscopy have been used to characterize the crystal structure and X-ray powder thermodiffractometry has been applied to determine the thermal expansion. Strikingly, we will show that the previously reported 'cubic' γ-GeP_2O_7 ($a \sim 22.86$ Å) displays the $3 \times 3 \times 3$ superstructure but it has much lower symmetry being monoclinic or triclinic.

EXPERIMENTAL

Syntheses

α-$Ge(HPO_4)_2 \cdot H_2O$, which will be hereafter referred to as α-GeP, was prepared hydrothermally in a Teflon-lined PARR autoclave with a free volume of 45 mL. α-GeP was obtained by heating a mixture of 0.8472 g GeO_2, 18.71 g H_3PO_4 (85% w/w), and 5.83 g of H_2O at 125°C for 7 days. The overall reactive molar ratios, Ge:P:H_2O, were 1:20:60. The resulting white solid was centrifuged, washed with water several times, and finally washed with acetone. α-GeP_2O_7 was synthesized by heating α-GeP at 800°C for 6 h.

γ-GeP_2O_7 was prepared as single phase at high temperature and pressure by using a piston-cylinder press (Rockland Research Co.). To do so, protocrystalline α-GeP_2O_7 was put into a gold capsule, sealed, and placed in a graphite heater. The pressure was set to 20 kbar and the temperature was held at 1000°C for 1 h. Then, the sample was quenched to room temperature and finally, pressure was released. γ-GeP_2O_7 was also prepared at ambient pressure by heating α-GeP at 1080°C for 1 day but it contains impurity phases. A purer γ-GeP_2O_7 sample was obtained at ambient pressure as follows. A slurry mixture of GeO_2 (1 g) and polyphosphoric acid (Aldrich 3 g) was heated at 500°C for 2.5 h.

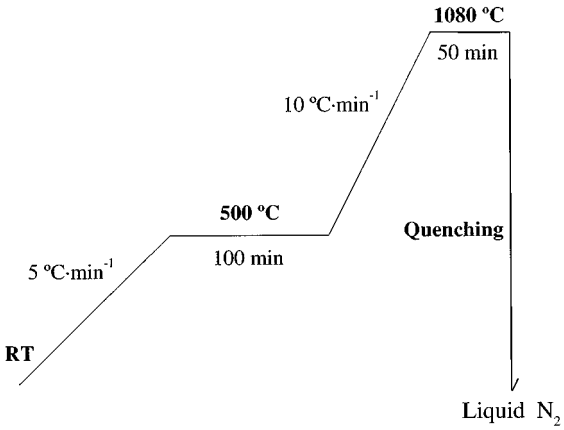

SCHEME 1. Synthetic route to obtaining crystalline γ-GeP_2O_7 at ambient pressure.

The resulting solid was cooled to room temperature, washed with water, dried, and pelletized. The pellet underwent the thermal treatment indicated in Scheme 1. After this treatment, the sample was examined by X-rays and was found to consist of a major phase, γ-GeP_2O_7, and a minor one, $Ge_5O(PO_4)_6$. Then, the mixture was pelletized again and the upper surface was covered with a drop of polyphosphoric acid. The same thermal treatment was applied which yielded γ-GeP_2O_7 (~95%).

β-GeP_2O_7 was obtained as a single phase. To do so, a pellet of α-GeP_2O_7 was covered with a drop of polyphosphoric acid to avoid the loss of P_2O_5. The sample underwent the thermal treatment showed in Scheme 1 but at lower temperature (the maximum temperature was 980°C instead of 1080°C). The quenching was carried out in water which was used to wash the excess of phosphorus. $Ge_5O(PO_4)_6$ was obtained as a single phase by heating α-GeP at 1200°C for $\frac{1}{2}$ day.

Techniques

Room temperature X-ray powder diffraction. X-ray powder diffraction patterns for all samples were collected on a Siemens D-5000, automated diffractometer using graphite-monochromated Cu$K\alpha_{1,2}$ radiation for phase identification and for monitoring of the chemical reactions. The $3 \times 3 \times 3$ superstructure of γ-GeP_2O_7 was studied using strictly monochromatic Cu$K\alpha_1$ radiation, $\lambda = 1.5405981$ Å, obtained from a Ge (111) primary monochromator, in an Philips X'PERT diffractometer. The pattern was scanned over the angular range, 10–120° (2θ), with a step size of 0.02° and counting for 25 s per step.

Variable temperature X-ray powder diffraction. The powder thermodiffractometric studies of α-GeP and γ-GeP_2O_7 were carried out in air on a Siemens D-5000 with

a second goniometer permanently equipped with an HTK10 heating chamber. The samples were packed over the Pt strip that acts both as the heating system and the holder. The patterns were scanned over the angular range, 6–38° (2θ), with a step size of 0.03° and counting for 3 and 10 s per step for α-GeP and γ-GeP_2O_7, respectively. The appropriate heating temperatures were selected by using the Diffract AT software. A delay of 10 min was applied before collection of any pattern to allow for transformations to take place.

^{31}P MAS-NMR spectra. ^{31}P MAS-NMR spectra were obtained at room temperature in a MSL 400 Bruker spectrometer at 161.96 MHz. γ- and β-GeP_2O_7 were spun at $\sim$10 kHz and $Ge_5O(PO_4)_6$ at $\sim$4 kHz and the spectra taken after $\pi/2$ pulse irradiation (4 μs). A time interval of 2–90 s between successive scans was chosen and the number of scans was $\sim$20. The ^{31}P chemical shifts are given relative to 85% aq H_3PO_4.

RESULTS AND DISCUSSION

The thermal behavior of α-GeP, which belongs to the α-$Zr(HPO_4)_2 \cdot H_2O$ type structure (14), was studied by DTA-TG and powder thermodiffractometry. The DTA-TG curves agree with those reported early but we detect four endotherms in the water loss region centered at 310, 410, 480, and 580°C, instead of the three endotherms observed by Chernorukov *et al.* (12). Figure 1 shows the powder thermodiffractometry of α-GeP at selected temperatures, which was carried out under He flow. α-$Ge(HPO_4)_2 \cdot H_2O$ is stable up to 250°C and above that temperature loses the hydration water to yield $Ge(HPO_4)_2$. This compound is stable up to 500°C. However, $Ge(HPO_4)_2$ undergoes a polymorphic transformation at 450°C which is evident in the thermodiffractometric study as new diffraction peaks appear in the 450°C pattern. Above 550°C, the hydrogenphosphate groups condense to yield α-GeP_2O_7 which is stable up to 900°C. However, its powder diffraction pattern changes slightly with temperature being quasi-amorphous at 650°C and with sharper peaks (larger long-range order) at 950°C. The relationship in the position of some diffraction peaks with those of the parent layered compound suggest that the structures are similar. It has also been suggested that a topotactic dehydration of $M(HPO_4)_2 \cdot H_2O$ (M = Ti, Zr) yields protocrystalline layered MP_2O_7 at low temperatures, $\sim$600°C (15). The peaks due to β-GeP_2O_7 starts to develop in the pattern collected at 1000°C. At 1050°C, the powder pattern contains the peaks characteristic of β-GeP_2O_7 and γ-GeP_2O_7. At 1100°C, the main peaks of $Ge_5O(PO_4)_6$ begin to appear which means that the sample is starting to release P_2O_5. $Ge_5O(PO_4)_6$ is isostructural with $Si_5O(PO_4)_6$ that can be prepared at low temperatures and it is stable up to 1000°C (16).

The powder pattern of α-GeP heated at 980°C in a crucible for 6 h matches that of PDF 82-0829, which corresponds to β-GeP_2O_7, although the main peak of γ-GeP_2O_7 was also evident in the pattern. β-GeP_2O_7, transforms on heating to γ-GeP_2O_7, although before this transformation is finished, $Ge_5O(PO_4)_6$ starts to appear. The powder pattern of α-GeP heated at 1200°C in a crucible matches that of PDF 71-0679 [$Ge_5O(PO_4)_6$]. This final thermal treatment

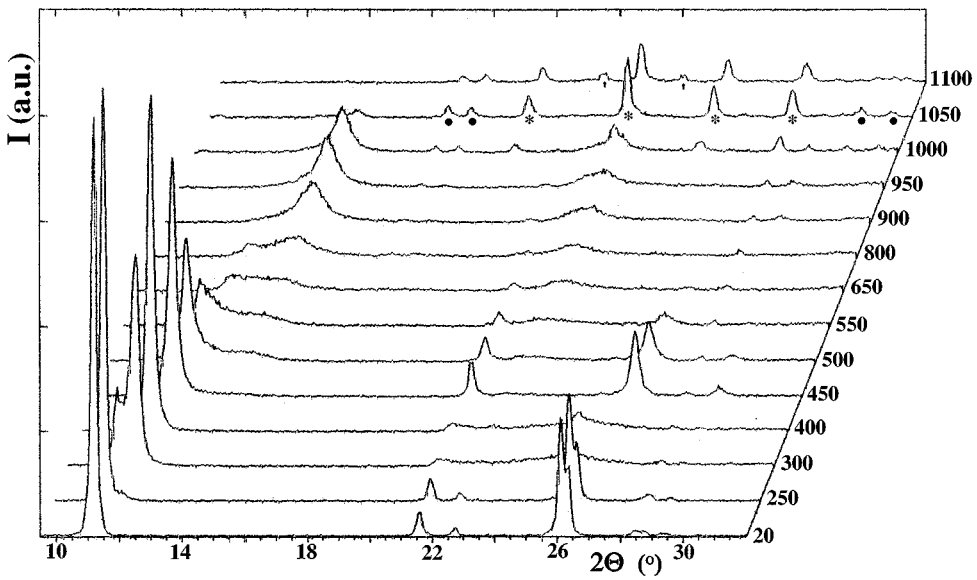

FIG. 1. X-ray powder patterns for α-$Ge(HPO_4)_2 \cdot H_2O$ with temperature (°C) in the z axis. Main peaks for β-GeP_2O_7 (●), γ-GeP_2O_7 (*), and $Ge_5O(PO_4)_6$ (′) are labeled.

was not carried out in the HTK10 heating chamber to avoid possible P_2O_5 contamination. Prolonged heating of any GeP_2O_7 sample above 1200°C yields $Ge_5O(PO_4)_6$. The preparation of γ-GeP_2O_7 is more difficult than that of many other "cubic" $M^{IV}P_2O_7$ compounds because this phase is not stable at high temperatures. All attempts to prepare it as a single phase at ambient pressure and different temperatures were unsuccessful as it was contaminated with the low-temperature phase, β-GeP_2O_7, or with the high-temperature thermal decomposition compound, $Ge_5O(PO_4)_6$.

As γ-GeP_2O_7 has higher density than the other well characterized polymorph, β-GeP_2O_7, high-pressure synthesis appeared suitable to prepare it; moreover, the high pressure also avoids the release of P_2O_5. The precursor for this procedure was α-GeP_2O_7. γ-GeP_2O_7 was reproducibly prepared as a crystalline single phase with tiny, well-faceted single crystals, by heating under pressure. These crystals did not extinguish light as a whole in the polarizing microscope under crossed polaroids, but rather they seemed to contain many small domains, as well as other defects. Attempts to collect a good data set with a CCD-equipped single crystal diffractometer were unsuccessful, as the diffraction spots were not indexable in terms of a unique set of basis vectors. This was likely due to the poor quality of the crystals. γ-GeP_2O_7 could also be prepared at ambient pressure as indicated above, but it contains impurity phases.

The peaks in the Cu$K\alpha_{1,2}$ powder pattern of γ-GeP_2O_7 have shoulders which cannot be justified with the previously reported cubic $3\times3\times3$ unit cell. To avoid the errors and correlations arising from the $K\alpha_{1,2}$ doublets, a powder pattern with strictly monochromatic Cu$K\alpha_1$ radiation was recorded (Fig. 2). The inset to that figure shows the splitting of the (111) substructure reflection, which indicates that the symmetry is monoclinic (or lower). Other substructure peaks are also split. Many small intensity diffraction peaks are also visible that can *only* be indexed with the $3\times3\times3$

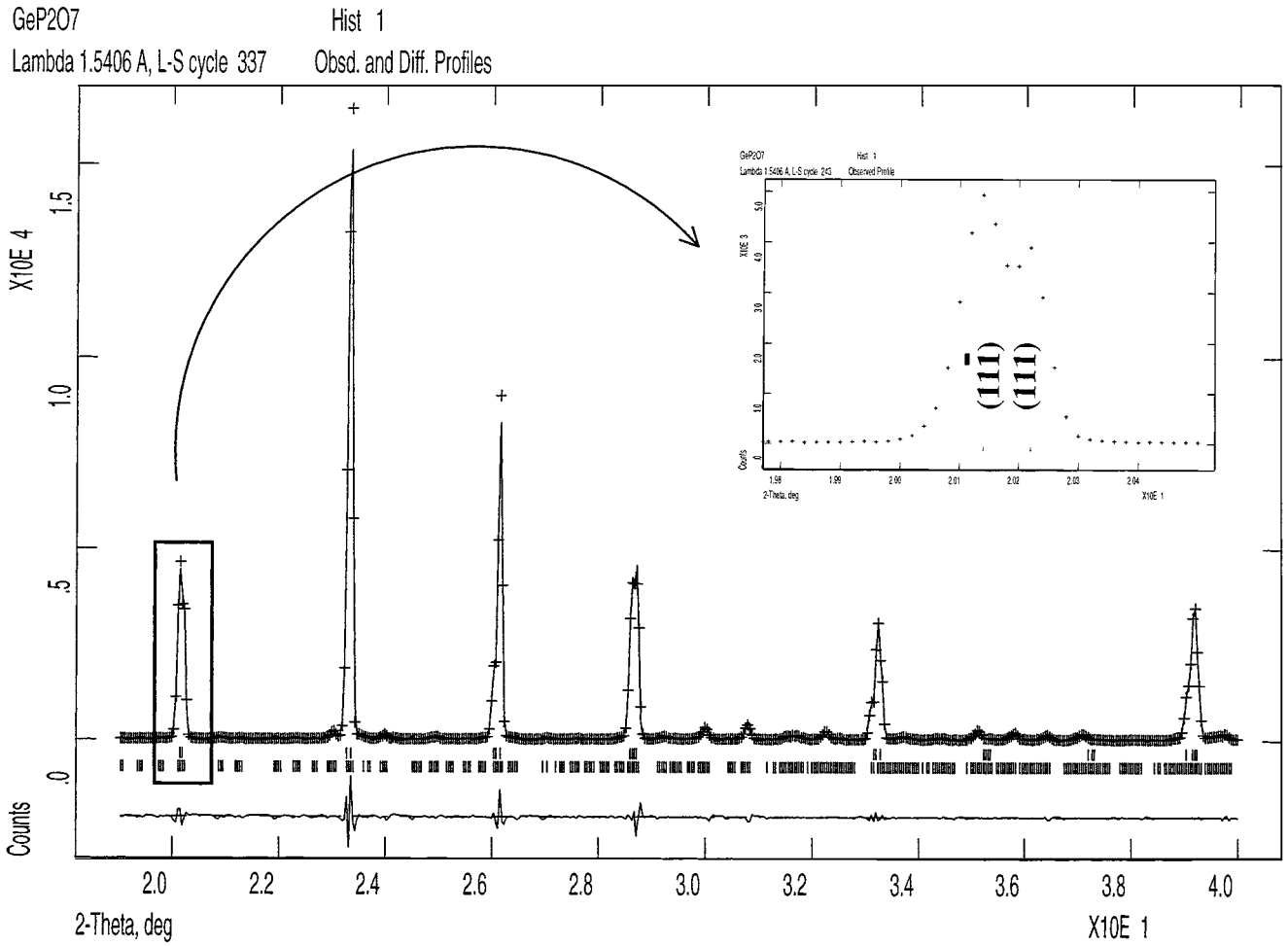

FIG. 2. Selected region of Rietveld plot (le Bail's fit) of the Cu$K\alpha_1$ powder pattern for γ-GeP_2O_7. Tics show the allowed Bragg peaks for the monoclinic $\sim7.6\times7.6\times7.6$ Å subcell (top) and the $\sim23\times23\times23$ Å supercell (bottom). The splitting of the (111) substructure peak is shown in the inset.

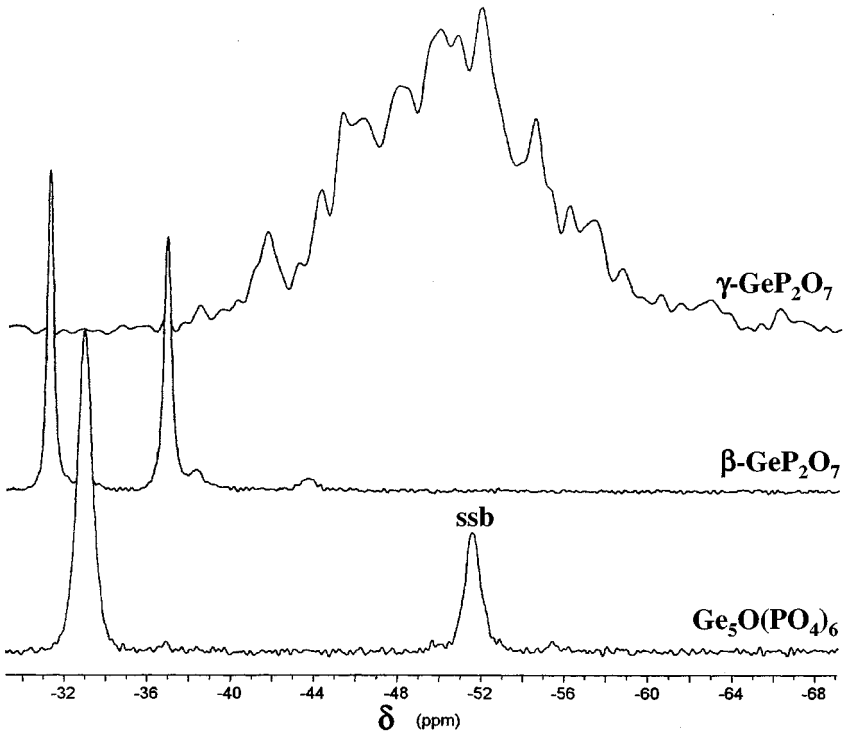

FIG. 3. ^{31}P MAS-NMR spectra for γ-GeP_2O_7 (top), β-GeP_2O_7 (center), and $Ge_5O(PO_4)_6$ (bottom). ssb denotes spinning side band associated with the rotation of the sample.

supercell. Hence, γ-GeP_2O_7 crystallizes in a monoclinic $3 \times 3 \times 3$ cell. Smaller related cells were tested but they did not index all superstructure peaks. The pattern was fitted by the Rietveld method (17) using the GSAS suite of programs (18) but without structural model (Le Bail's fit (19)). The resulting refinement was very good: $a = 22.8647(4)$ Å, $b = 22.8783(4)$ Å, $c = 22.9429(4)$ Å, $\beta = 90.328(1)^\circ$, $V = 12001.3(4)$ Å^3, $P2_1/c$, with $R_{WP} = 11.5\%$. No attempts to solve or refine this structure from powder diffraction data were carried out. It should be noted that the description of the structure in $P2_1/c$ requires the following crystallographically independent atoms: 28 Ge (two in special positions), 54 P, and 190 O (two in special positions). This structure is too complex to be studied by powder diffraction methods. Single-crystal data are needed but, so far, we have been unable to grow crystals good enough to yield meaningful data.

The monoclinic $3 \times 3 \times 3$ cell of γ-GeP_2O_7 is not the result of the high-pressure synthesis. The ambient pressure preparations of γ-GeP_2O_7 also showed the splitting in the patterns. The low symmetry is confirmed by the MAS-NMR spectrum shown in Fig. 3. NMR spectra were collected for both types of preparations, ambient and high-pressure, and they are quite similar. Here, we report the spectrum from single-phase γ-GeP_2O_7. This low symmetry is in agreement with previous observations (9) for MoP_2O_7 and it may explain the problems encountered when trying to describe the structure of some MP_2O_7 compounds such us $M = Zr$ (6). In this last case, the reported structure has many unrealistic bond distances, angles, and temperature factors. The structural relationship of the pseudo-cubic MP_2O_7 (M = Ge, Sn, Pb) and (M = Ti, Zr, Hf) families studied by with Cu$K\alpha_1$ and neutron powder diffraction and ^{31}P MAS-NMR spectroscopy will be the subject of a forthcoming paper.

In Fig. 3, the ^{31}P MAS-NMR spectra for $Ge_5O(PO_4)_6$, β-GeP_2O_7, and γ-GeP_2O_7 are shown. The profile for $Ge_5O(PO_4)_6$ contains a single resonance at -32.9 ppm, which is in agreement with the structure as there is a unique crystallographically independent phosphate group. The spectrum for β-GeP_2O_7 contains two resonances at -31.3 and -36.9 ppm, which also agrees with the structure as there is a single crystallographically independent pyrophosphate group with two different PO_4 tetrahedra. It is worth emphasizing that these values are displaced from the values observed for other pyrophosphate groups in MP_2O_7 (1, 7). For β-GeP_2O_7, the two detected NMR lines are shifted toward the values detected in Ge-orthophosphates (-32/45 ppm). This shift may be due to the small P–O–P value of the bridging angle which is 126.5°. For γ-GeP_2O_7, the

NMR spectrum displays a considerable complexity and NMR lines are spread over the $-42/-62$ ppm range. Many peaks, more than 35, were observed in the profile which indicates the existence of many crystallographically independent phosphorus atoms. More nonresolved components can be hidden in this spectrum. This observation is in agreement with the low symmetry measured in the diffraction study.

Three possible monoclinic space groups can be obtained from $Pa\bar{3}$ by removing symmetry elements: $P2_1/c$, $P2_1$, and Pc. As noted in Fig. 4 of Ref. (1), the number of independent pyrophosphate groups are 54, 108, and 108, respectively. In $P2_1$ and Pc space groups, no linear P–O–P groups are required but two are needed in $P2_1/c$. Hence, although our powder diffraction data and ^{31}P MAS-NMR spectrum for γ-GeP_2O_7 are compatible with $P2_1/c$, we cannot rule out a lower symmetry. It is remarkable that a compound with such simple stoichiometry, GeP_2O_7, contains at least 54, maybe even 108, different PO_4 groups in its unit cell. Such structure gives very complex X-ray diffraction and ^{31}P MAS-NMR profiles.

The thermal expansion behavior of γ-GeP_2O_7 has been characterized by Cu$K\alpha_{1,2}$ laboratory thermodiffractometry. The compounds remains monoclinic with the $3\times3\times3$ superstructure up to the highest investigated temperature, 750°C. Substructure peaks are split and some diffraction peaks are displaced more than others, on heating, as expected in a noncubic material. However, it should be noted that determining the thermal evolution of γ-GeP_2O_7 quantitatively is not straightforward. The unit cell is very complex with many overlapped peaks that led to divergence in the Le Bail's fits because there are many correlations. The sample alignment is not ensured as the height of the sample layer cannot be properly controlled. This results in a zero shift-like error. Furthermore, the sample height can slightly change during the experiment. The peaks due to the Cu$K\alpha_2$ radiation also increase the errors. To avoid divergences, we used the approximation of fitting the Cu$K\alpha_{1,2}$ patterns taken at different temperatures with the monoclinic subcell. As examples, we give the cell edges at three selected temperatures to show the slightly anisotropic thermal behavior: $a = 7.60$, 7.62, and 7.70 Å; $b = 7.61$, 7.64, and 7.67 Å; and $c = 7.64$, 7.67, and 7.67 Å for 20, 400, and 750°C, respectively.

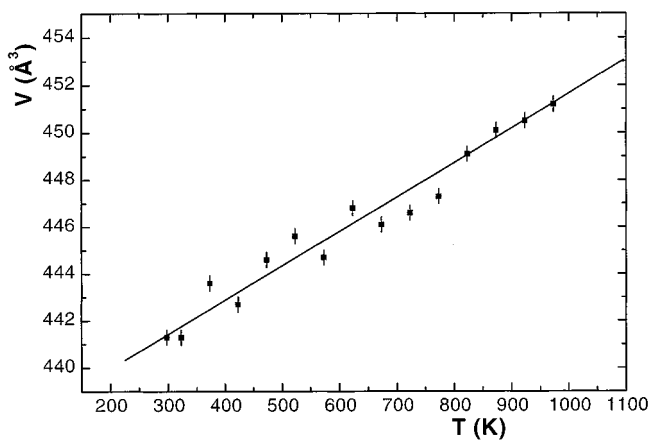

FIG. 4. Thermal expansion for γ-GeP_2O_7 expressed as the variation of the volume of the monoclinic subcell with temperature, obtained from Cu$K\alpha_{1,2}$ powder diffraction data.

Under the described conditions and approximations, the results of these refinements are given in Fig. 4. The cell behavior can be fitted with $V = 437.0(6) + 0.0146(8)T$. This result is close to that obtained for M = Ti, $V = 483.5(3) + 0.0141(6)T$. Hence, γ-MP_2O_7 (M = Ge, Ti) shows positive thermal expansion coefficients, α_V, being 33 10^{-6} and 29 10^{-6} K^{-1} for M = Ge and Ti, respectively. The thermodiffractometry of γ-GeP_2O_7 is similar to that of TiP_2O_7 where there is no transition to a powder pattern without superstructure peaks at relatively low temperatures. However, such transition was clearly observed (1) in ZrP_2O_7 and has been reproduced by us and others (20), with a remarkable reduction of the thermal expansion.

ACKNOWLEDGMENTS

This work was supported by the research grants MAT97-326-C4-4 and MAT98-1053-004-03 of the CICYT.

REFERENCES

1. V. Korthuis, N. Khosrovani, A. W. Sleight, N. Roberts, R. Dupree, and W. W. Warren, *Chem. Mater.* **7,** 412 (1995).
2. G. R. Levi and G. Peyronel, *Z. Kristallogr.* **92,** 190 (1935).
3. H. Völlenkle, A. Wittmann, and H. Nowotny, *Monatsh. Chem.* **94,** 956 (1963).
4. L. O. Hagman and P. Kierkegaard, *Acta Chem. Scand.* **23,** 327 (1969); M. Chaunac, *Bull. Soc. Chim. Fr.* 424 (1971); C-H. Huang, O. Knop, D. A. Othen, F. W. D. Woodhams, and R. A. Howie, *Can. J. Chem.* **73,** 79 (1975).
5. E. Tillmanns, W. Gebert, and W. H. Baur, *J. Solid State Chem.* **7,** 69 (1973).
6. N. Khosrovani, V. Korthuis, A. W. Sleight, and T. Vogt, *Inorg. Chem.* **35,** 485 (1996).
7. J. Sanz, J. E. Iglesias, J. Soria, E. R. Losilla, M. A. G. Aranda, and S. Bruque, *Chem. Mater.* **9,** 996 (1997).
8. R. L. Withers, J. S. O. Evans, J. Hanson, and A. W. Sleight, *J. Solid State Chem.* **137,** 161 (1998); J. S. O. Evans, J. C. Hanson, and A. W. Sleight, *Acta Crystallogr. B* **54,** 705 (1998).
9. R. C. Haushalter and L. A. Mundi, *Chem. Mater.* **4,** 31 (1992).
10. A. E. Malshikov, O. V. Egorova, and I. A. Bondar, *Russ. J. Inorg. Chem.* **33,** 722 (1988).
11. H. Mayer and H. Völlenkle, *Monatsh. Chem.* **103,** 1560 (1972).
12. N. G. Chrenorukov, I. R. Mochalova, E. P. Moskvichev, and G. F. Sibrina, *Zhur. Prikl. Khim.* **50,** 1618 (1977).
13. U. Kaiser and R. Glaum, *Z. Anorg. Allg. Chem.* **610,** 1755 (1994).
14. J. M. Troup and A. Clearfield, *Inorg. Chem.* **16,** 3311 (1977).

15. (a) U. Constantino and A. La Ginestra, *Thermochem. Acta* **58,** 179 (1982); (b) D. M. Poojary, R. B. Borade, F. L. III Campbell, and A. Clearfield, *J. Solid State Chem.* **122,** 106 (1994).
16. D. M. Poojary, R. B. Borade, and A. Clearfield, *Inorg. Chim. Acta* **208,** 23 (1993).
17. H. M. Rietveld, *J. Appl. Crystallogr.* **2,** 65 (1969).
18. A. C. Larson and R. B. Von Dreele, Los Alamos National Lab. Rep. LA-UR-86-748. Los Alamos National Laboratory, Los Almos, NM, 1994.
19. A. Le Bail, H. Duroy, and J. L. Fourquet, *Mater. Res. Bull.* **23,** 447 (1988).
20. W. I. F. David, J. S. O. Evans, A. W. Sleight, and R. M. Ibberson, ISIS experimental report (1999).